Small Broadband Receiving Antenna Using a Fabry-Perot Etalon

Gabriel V. Meyer and Armin Wittneben

Abstract— **A novel concept for a broadband electric-field (E-field) receiving antenna is proposed. The reactive near field, induced by an impinging E-field, of a very short, short-circuited dipole is picked-up with the aid of an electro-optical modulator. The modulator is designed as a Fabry-Perot etalon. The laser light guided in the etalon is modulated proportionally to the near field of the dipole. The advantage of the etalon is to considerably increase the sensitivity of the antenna compared to known electro-optic probes. It is shown analytically for an ellipsoidal dipole and numerically for a cylindrical dipole, that only the quasi electrostatic terms of the dipole field are relevant. Important is the optimal choice of the material of the modulator. Since the linear electro- optical effect is used, best results are achieved if the index ellipsoid of the material parameters does not rotate under the influence of an external field but only varies its size. Such behaviour is found in materials as e.g. $LiNbO_3$ and poled polymers. Because of reflections, a second parameter of concern is the permittivity of the modulator base material. Polymers are the most promising materials known today for this type of antennas.**

The proposed antenna may either be used as broadband E-field probe or receiving antenna. It features low coupling because of the small size and the fibre optic feeding, low signal attenuation in the feeding and large bandwidth. This type of antennas is therefore optimally suited for distributed UWB antenna systems where only one way wireless communication is necessary.

***Index Terms*—Antenna, electro-optic antenna, etalon.**

I. Introduction

An EM-field probe and a receiving antenna both act as a wave-type-transformer from radiated to guided waves. Compared to a classical, reciprocal antenna the former are non-reciprocal elements. Probe and receiving antenna are therefore treated as synonyms. The physical characteristics of the field captured with the type of electro-optic E-field antenna introduced in this paper is the one-dimensional electric field component parallel to the dipole axis.

Previous work on field probes using electro-optic transformation has been concentrated on applying modulators at the feeding point of dipoles. To the knowledge of the authors modulators only have been used in the form of Mach-Zehnder interferometer in numerous variations [1]; over 100 patents can be found in the literature. The Mach-Zehnder interferometer should be better replaced by a Fabry-Perot etalon, since the cavity of the etalon considerably increases the sensitivity of the structure. A further amplification of the impinging field is achieved by making use of the field concentration in the close proximity of the antenna structure. In this paper a solution is presented featuring minimal interaction between probe and impinging EM-field, by sacrificing some amount of the dynamic range.

Authors are with Communication Technology Laboratory, Sternwartstr. 7, ETH Zurich, CH-8092 Zurich, Switzerland (e-mail: gmeyer@nari.ee.ethz.ch)

Other remarkable solutions applying electro-optic effects use e.g. a Bragg-structure [2], sectorized electrodes and a Mach-Zehnder interferometer [3], a ring laser using the Faraday effect [4] or a Luneberg-lens to focus the EM-energy [5]. Also a polarizer-analyzer structure with a sphere of electro-optical material has been proposed [6].

The great advantage of the probe described in this paper is its small size, featuring a minimal interaction with the probe and the impinging field, as well as the possibility to realize two and three dimensional sensor arrays. With the aid of such structures the direction of arrival of far fields without ambiguity can be estimated as well as the structure of inhomogeneous EM-fields. In the following we concentrate on the theoretical basics for a small sized E-field probe using an etalon as an electro-optical transformer. Section II contains a short description of the principal construction of the near field probe. In section III the reactive near field of the probe is analyzed, section IV is devoted to the material properties for etalons and the characteristics of the probe such as the sensitivity, the bandwidth and the dynamic range. This is followed by conclusions and an outlook.

II. Construction of the Antenna

The E-field antenna consists of an electrical short, short-circuited dipole situated in the centre of a dielectric sphere. The form of the dipole presented in this study is chosen as a rotational ellipsoid (with length h and width b) for the purpose of easy analytical treatment. Any other known form of a dipole may be used but is not considered here. The outline of the probe is shown in Fig. 1. A Fabry-Perot etalon is placed directly on the surface of the dipole where locally the highest field strength is available. As will be shown in IIIB the most prominent E-field is induced at the surface of the dipole perpendicular to that surface and therefore is ideally suited to activate the etalon.

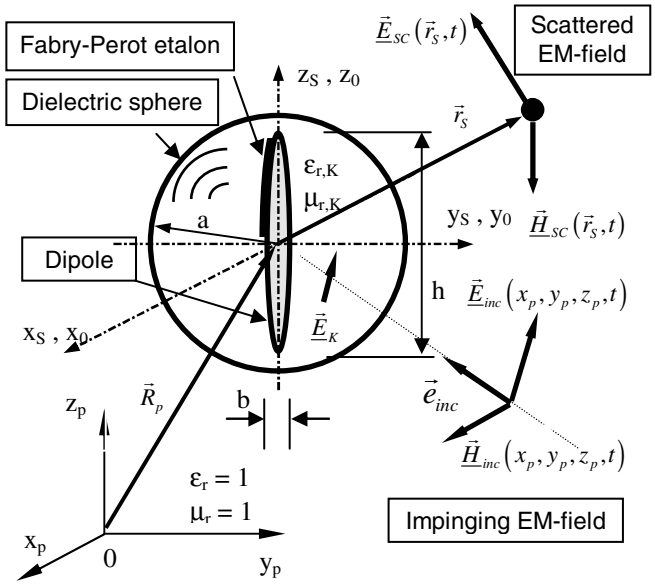

Fig. 1. The E-field antenna with dipole and Fabry-Perot etalon contained in a dielectric sphere.

The aim of the dielectric sphere with radius a and relative permittivity $\varepsilon_{r,K}$ is to reduce the gap between the material parameters of the etalon and the surroundings ($\varepsilon_r = 1$). The relative permeability μ_r is assumed to be 1 everywhere.

The dielectric sphere is not a prerequisite for the function of the sensor. However by optimising the material parameters of the etalon and the sphere the sensitivity of the probe may be increased.

III. The Reactive Near Field

A. Limit of the Near Field

The electromagnetic field distribution in the vicinity of a short thin dipole shall be considered in this paragraph. The dipole has the form of a prolate ellipsoid and is short circuited (no gap). In the following we concentrate on impinging far fields E_{inc} of the form:

$$\underline{\vec{E}}(x_0, y_0, z_0, t) = \underline{\vec{E}}(x_0, y_0, z_0) \cdot e^{-j\cdot\omega\cdot t} \tag{1}$$

where: $j \equiv \sqrt{-1}$; ω: angular frequency t: time and complex variables are underlined. It can be shown [7, 8] that among the different constraints to be fulfilled for the max. size of the antenna:

$$k\,a \le 0.3 \tag{2}$$

is the most stringent; where a is defining the smallest sphere comprising the antenna (see Fig. 1) and k is the wave number. In this case the difference between the assumed electro and magneto static fields and the real field is less than 10%. By varying the relative permittivity ε_r of the surrounding sphere we find an estimated maximum allowed dimension of the probe leading to a systematic error of less than 10% (see Fig. 2).

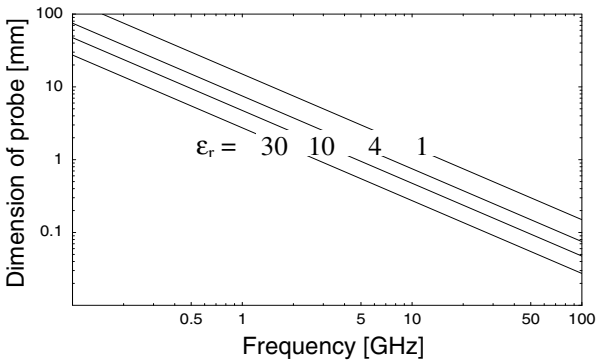

Fig. 2. Maximum dimension of the probe for the assumption of static field conditions.

B. Field Distribution in the Vicinity of the Dipole

As long as the length of the dipole h is less than a in eq. 2 the static field is dominant within the sphere a in Fig. 1. That means only the quasi-static field term is relevant for the modulation of the etalon.

We consider therefore the problem of an ellipsoidal dipole immersed in a TEM field with the E-field vector parallel to the main axis of the dipole. For ease of computation we choose a prolate spheroidal coordinate system (ζ , θ , ψ) as shown in Fig. 3.

Assuming an impinging field of the form:

$$\vec{E}_0 = \begin{bmatrix} E_x \\ E_y \\ E_z \end{bmatrix} = \begin{bmatrix} 0 \\ 0 \\ -E_0 \end{bmatrix} \tag{3}$$

We get for the scalar electric potential ϕ[9]:

$$\phi(\zeta,\theta,\psi) = \sum_{n=0}^{\infty} \left[B_n P_n \cosh(\zeta) + C_n Q_n \cosh(\zeta) \right] \cdot P_n \cos(\theta) \tag{4}$$

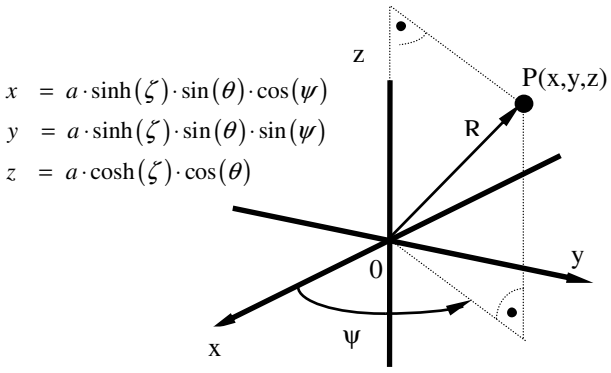

Fig. 3: Prolate spheroidal coordinate system.

where P_i indicate Legendre polynoms of the first kind, and Q_i of the second kind, respectively. The boundary conditions have to be satisfied and since the electrostatic field is proportional to the gradient of the scalar potential we get from (4) an expression for the electric field in the proximity of the dipole in case of parallel polarisation:

$$E_\zeta(\zeta,\theta,\psi) = -\frac{E_0 \cdot \cos(\theta)}{\sqrt{\left[\sinh(\zeta)\right]^2 + \left[\sin(\theta)\right]^2}} \cdot \left[\sinh(\zeta) - \frac{\cosh(\zeta_0)}{Q_1(\cosh(\zeta_0))} \cdot Q_1'(\cosh(\zeta)) \right]$$

$$E_\theta(\zeta,\theta,\psi) = \frac{E_0 \cdot \sin(\theta)}{\sqrt{\left[\sinh(\zeta)\right]^2 + \left[\sin(\theta)\right]^2}} \cdot \left[\cosh(\zeta) - \frac{\cosh(\zeta_0)}{Q_1(\cosh(\zeta_0))} \cdot Q_1(\cosh(\zeta)) \right] \tag{5}$$

$$E_\psi(\zeta,\theta,\psi) = 0; \qquad Q_1'(\cosh(\zeta)) = \frac{d}{d\zeta} Q_1(\cosh(\zeta))$$

On the surface of the dipole we deduce from (5) that only the component E_ζ exists.

Fig. 4 shows the increase of the field component E_ζ relative to the free field E_0. For the ratio of the short to the long axis of the dipole b/h = 0.01 this ratio varies between 100 to 1000 over about 2/3 of the extension of the dipole.

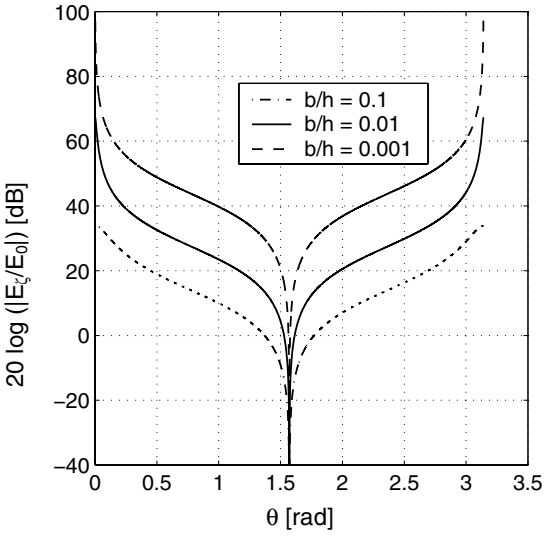

Fig. 4. Relative field strength increase at a surface line along the dipole.

The equipotential lines surrounding the dipole may be seen in Fig. 5. From this figure an estimate of the size of the surrounding dielectric sphere may be gained since the assumption of static field requires having parallel equipotential lines at the inner surface of the sphere.

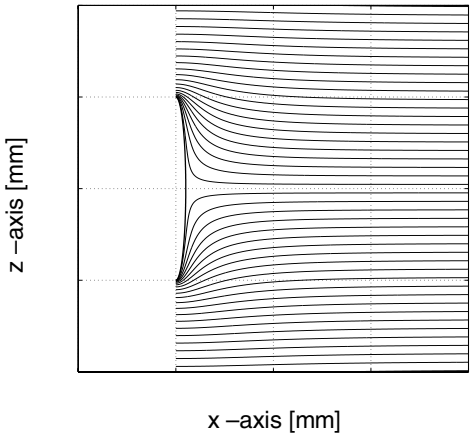

Fig. 5. Equipotential lines around the dipole with b/h=0.1

Numerical simulations have shown that the near field condition eq. 2 considerably can be relaxed and also that the ellipsoidal dipole can be replaced by a cylinder without introducing a significant error (see e.g. Fig. 6). The curves shown in Fig. 6 remain the same for the whole frequency range except for the vicinity of the dipole resonances ($h = i\,\lambda/2,\ i \in \{1,2,3,...\}$).

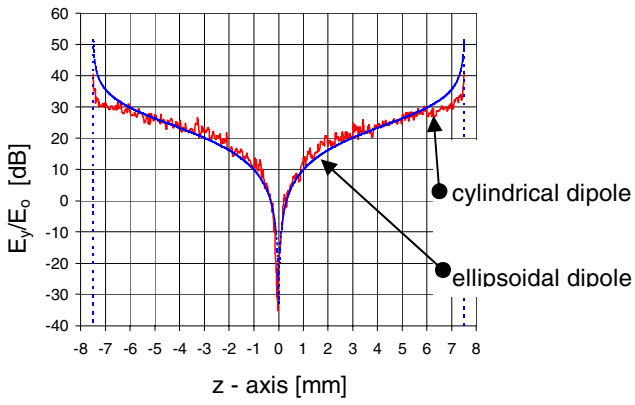

Fig. 6. E_y nearfield component along the perimeters of ellipsoidal resp. cylindrical dipoles of 15 mm length with b/h = 0.01 at a frequency of 100 MHz .

For an impinging electric far field perpendicular polarized to the main axis of the ellipsoidal dipole, the latter may be replaced by an infinitesimal cylinder. This is a reasonable assumption in case of a thin ellipsoid in the centre region of the dipole, but the effects of the ends are not considered. In a cylindrical coordinate system with the axes (r, β, z), it is known that the electrostatic field surrounding a conducting cylinder is given by:

$$E_r(r,\beta,z) = E_0 \cdot \left[\frac{b^2}{r^2}+1\right]\cdot\cos(\beta)$$

$$E_\beta(r,\beta,z) = E_0 \cdot \left[\frac{b^2}{r^2}-1\right]\cdot\sin(\beta) \qquad (6)$$

$$E_z(r,\beta,z) = 0$$

At the surface of the cylinder the only remaining field component is:

$$E_r(r=b,\beta,z) = E_0 \cdot 2 \cdot \cos(\beta) \qquad (7)$$

This means we only have a radial field component featuring a cosine function along the perimeter of the cylinder with a maximum value of two times the far field strength. Compared to the near field in case of parallel polarization (eq. 5 and Fig. 4) this leads to a cross polarization factor between 50 and 500. We conclude that only the field components parallel polarized to the antenna activate the electrooptic transducer.

IV. The Electrooptic Transducer

Instead of capturing the induced voltage at the gap of an antenna, the new idea realized with this probe is to make use of the enhanced quasistatic field in the proximity of the dipole periphery. This field directly acts on an electrooptical modulator consisting of an optical waveguide of length L_E (see Figs. 7 and 10). Optical modulators make use of the linear electrooptic effect [10]. The field E_ζ (see eq. 5) is applied directly to the optical modulator along its length L_E replacing the modulating signal in the normal operation of an electrooptic modulator. A considerable increase of the sensitivity of the modulator can be achieved by replacing the modulator with a Fabry-Perot etalon consisting of a modulator featuring two semipermeable mirrors at the ends.

A. *The Fabry-Perot etalon*

The principle of the Fabry-Perot etalon is shown in Fig. 7. A light wave E_{IN} guided by an optical fibre is impinging on the etalon from the left side. The etalon consists of two semipermeable mirrors and a piece of electro-optic material of the length L_E (modulator). An external EM field modulates the refractive index of the electro-optic material and therefore the propagation velocity of the light wave E_{IN}. The superposition of the multiple reflections and transmissions on mirror 1 leads to the resulting reflected light wave E_{OUT} in the optical fibre.

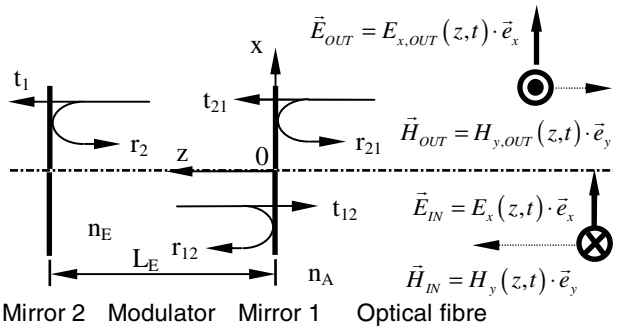

Fig. 7: Principle of the Fabry-Perot etalon.

The meaning of the symbols in Fig. 7 is the following:

- t_1 , t_{12} , t_{21}: value of the amplitude transmission coefficients at the mirror 1,
- r_2 , r_{12} , r_{21}: value of the amplitude reflection coefficients at the mirrors,
- n_E: refractive index of the modulator base material,
- n_A: refractive index of the optical fibre,
- L_E: length of the etalon

The etalon may be approximated by a linear dispersionless system and therefore Fourier techniques are applicable. Given the impulse response $h_{Etalon\text{-}R}(t)$ respective the transfer function $H_{Etalon\text{-}R}(\omega)$ at the mirror 1 or at z = 0 , in Fig. 7, the field strength resulting from the superposition of plane waves is given as:

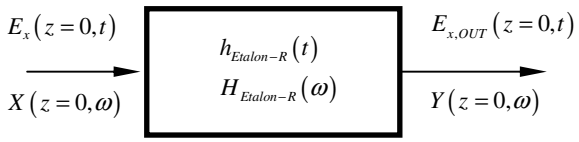

$$E_{x,OUT}(z=0,t) = r_{21}\cdot E_x(z=0,t) \quad + \quad + \quad [t_{12}\cdot t_{21}\cdot r_2]\cdot\sum_{m=0}^{\infty}[r_{12}\cdot r_2]^m\cdot E_x(z=0,t-2\cdot[m+1]\cdot\tau_E) \tag{8}$$

featuring a Fouriertransform Y of:

$$Y(z=0,\omega) = r_{21}\cdot X(z=0,\omega) \quad + \quad [t_{12}\cdot t_{21}\cdot r_2]\cdot \sum_{m=0}^{\infty}[r_{12}\cdot r_2]^m\cdot X(z=0,\omega)\cdot e^{-j\cdot\omega\cdot 2\cdot[m+1]\cdot\tau_E}$$

$$\Rightarrow Y(z=0,\omega) = \left[r_{21} \quad + \quad t_{12}t_{21}r_2e^{-j\cdot\omega\cdot 2\cdot\tau_E}\cdot\frac{1}{1-r_{12}r_2e^{-j\cdot\omega\cdot 2\cdot\tau_E}}\right]\cdot X(z=0,\omega) \tag{9}$$

where the transition time τ_E is given by:

$$\tau_E = \frac{L_E}{c_0}\cdot n_E$$

The frequency response of the etalon now may be computed from:

$$H_{Etalon-R}(\omega) = \frac{Y(z=0,\omega)}{X(z=0,\omega)} = r_{21} + t_{12}t_{21}r_2\cdot\frac{e^{-j\cdot\omega\cdot 2\cdot\tau_E}}{1-r_{12}r_2e^{-j\cdot\omega\cdot 2\cdot\tau_E}} \tag{10}$$

resp. for the intensities of the light wave:

$$\left|H_{Etalon-R}(\omega)\right|^2 = [r_{21}]^2 + \frac{2\cdot r_{21}\cdot t_{12}\cdot t_{21}\cdot r_2\cdot[\cos(\omega\cdot 2\cdot\tau_E)-r_{12}\cdot r_2]+[t_{12}\cdot t_{21}\cdot r_2]^2}{1-[r_{12}\cdot r_2]\cdot 2\cdot\cos(\omega\cdot 2\cdot\tau_E)+[r_{12}\cdot r_2]^2}$$

Assuming a monochromatic TEM light wave E_{IN} (see Fig. 7) the reflection coefficient R is also given by the intensity of the reflected wave I_R relative to the intensity of the impinging light I_{IN}. With the free space light wavelength λ_0 and the condition of the conservation of the energy:

$$t_{21} = t_{12} \quad ; \quad r_{21} = -r_{12} \quad ; \quad [t_{21}]^2 + [r_{21}]^2 = 1$$

we finally have:

$$R = \frac{I_R}{I_{IN}} = [r_{21}]^2 + \frac{2r_{21}[t_{12}]^2 r_2\left[\cos\left(4\pi\frac{L_E}{\lambda_0}n_E\right)+r_{21}r_2\right]+[t_{21}]^4[r_2]^2}{1+[r_{21}r_2]2\cos\left(4\pi\frac{L_E}{\lambda_0}n_E\right)+[r_{21}r_2]^2} \tag{11}$$

Interesting for the application of modulators is the sensitivity of R to small changes of the refractive index Δn: $R(n_{E0}+\Delta n)$

$$R(n_{E0}+\Delta n) \quad \approx \quad R(r_{21},r_2,t_{12},L_E,\lambda_0,n_{E0}) \quad + \quad + \frac{d}{dn_E}R(r_{21},r_2,t_{12},L_E,\lambda_0,n_E)\Big|_{n_E=n_{E0}}\cdot\Delta n \tag{12}$$

The computed sensitivity of the etalon is shown in Fig. 8 assuming $r_2 = -r_{21}$ and introducing the variable Λ:

$$\Lambda = 4\cdot\pi\cdot\frac{L_E}{\lambda_0}\cdot n_{E0} \tag{13}$$

The etalon has a 2π periodic reflection behaviour in the form of a filter. With increasing reflection r_2 at the end of the etalon the transmission region gets smaller and steeper. In addition the sensitivity of the etalon to small changes of the refractive index increases considerably. With increasing length of the etalon L_E, also the sensitivity increases.

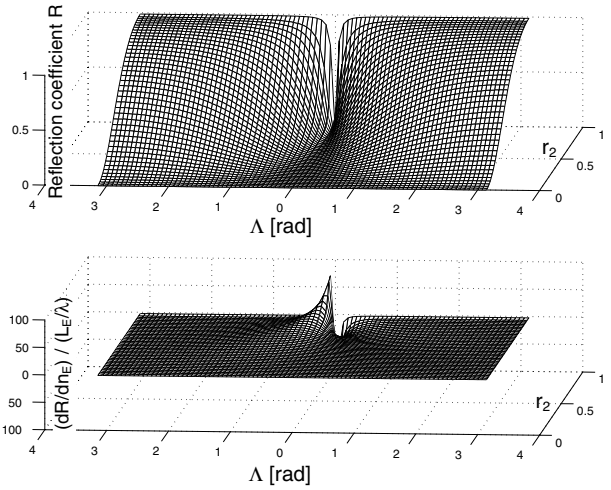

Fig. 8: Characteristics of the reflection coefficient and the sensitivity as a function of the reflection at the end of the etalon and some characteristic measures of the etalon Λ.

B. The linear electrooptic effect

If a material shows a linear dependency between an applied electric field and the optical refractive index it is called a linear electrooptic material. The linear electrooptic effect only exists in crystals that do not possess inversion symmetry. The propagation characteristics in crystals are fully described by means of the index ellipsoid (see Fig. 9).

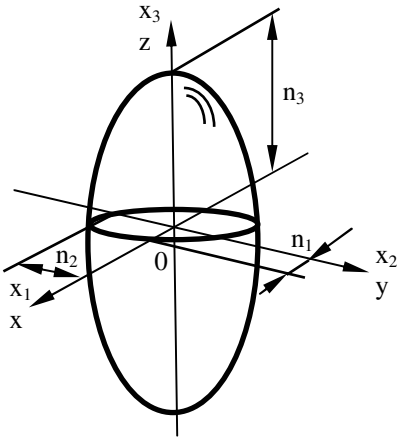

Fig. 9: Index ellipsoid with principal axes x_1, x_2 and x_3 and the corresponding principal refractive indices n_1, n_2 and n_3.

The index ellipsoid may be expressed as [10]:

$$\frac{[x_1]^2}{[n_1]^2} + \frac{[x_2]^2}{[n_2]^2} + \frac{[x_3]^2}{[n_3]^2} = 1 \tag{14}$$

Given an external electric field E:

$$\vec{E} = \begin{bmatrix}E_x\\E_y\\E_z\end{bmatrix} = \begin{bmatrix}E_1\\E_2\\E_3\end{bmatrix}$$

the index ellipsoid changes according to:

$$1 = \eta_1(E_1,E_2,E_3)\cdot[x_1]^2 + \eta_2(E_1,E_2,E_3)\cdot[x_2]^2 + \\ +\eta_3(E_1,E_2,E_3)\cdot[x_3]^2 + 2\cdot\eta_6(E_1,E_2,E_3)\cdot x_1\cdot x_2 + \\ +2\cdot\eta_5(E_1,E_2,E_3)\cdot x_1\cdot x_3 + 2\cdot\eta_4(E_1,E_2,E_3)\cdot x_2\cdot x_3 \tag{15}$$

where for the coefficients η only the linear terms are taken into account. The equations for the coefficients of the index ellipsoid (eq. 15) can be represented in form of a matrix:

$$\begin{bmatrix}\eta_1(E_1,E_2,E_3)\\ \eta_2(E_1,E_2,E_3)\\ \eta_3(E_1,E_2,E_3)\\ \eta_4(E_1,E_2,E_3)\\ \eta_5(E_1,E_2,E_3)\\ \eta_6(E_1,E_2,E_3)\end{bmatrix}=\begin{bmatrix}\frac{1}{[n_1]^2}\\ \frac{1}{[n_2]^2}\\ \frac{1}{[n_3]^2}\\ 0\\ 0\\ 0\end{bmatrix}+\left\{\begin{bmatrix}m_{11}&m_{12}&m_{13}\\ m_{21}&m_{22}&m_{23}\\ m_{31}&m_{32}&m_{33}\\ m_{41}&m_{42}&m_{43}\\ m_{51}&m_{52}&m_{53}\\ m_{61}&m_{62}&m_{63}\end{bmatrix}\cdot\begin{bmatrix}E_1\\ E_2\\ E_3\end{bmatrix}\right\} \quad (16)$$

The coefficients m_{ik} are called the linear electro-optic coefficients. As can be expected in a general case from eq. 15, the index ellipsoid is changed and rotated under the influence of an external field. This results in cross terms and a split of the impinging field in ordinary and extraordinary rays, what is called birefringence. Anisotropic materials suitable for modulation purposes in information carrying systems must be approximated by an index ellipsoid according to:

$$1=\eta_1(E_1,E_2,E_3)\cdot[x_1]^2+\eta_2(E_1,E_2,E_3)\cdot[x_2]^2+\eta_3(E_1,E_2,E_3)\cdot[x_3]^2 \quad (17)$$

Provided the following inequations are valid:

$$[m_{i1}\cdot E_1+m_{i2}\cdot E_2+m_{i3}\cdot E_3]\cdot[n_i]^2\ll 1 \quad ;i\in\{1,2,3\} \quad (18)$$

the change of the refractive indices under the influence of an external electromagnetic field of such materials may be approximated with:

$$n_i(E_1,E_2,E_3)\approx n_i+\Delta n_i \quad ;$$
$$with\ \Delta n_i=-\frac{1}{2}\cdot[m_{i1}\cdot E_1+m_{i2}\cdot E_2+m_{i3}\cdot E_3]\cdot[n_i]^3;\ i\in\{1,2,3\} \quad (19)$$

In the literature two materials can be found suitable for Fabry-Perot etalons: $LiNbO_3$ and poled polymers. Widely used today is $LiNbO_3$ featuring an electrooptic tensor of [11, 12]:

$$m_{LiNbO_3}(\lambda_0=633nm)=\begin{bmatrix}0&-3.4&8.6\\ 0&3.4&8.6\\ 0&0&30.8\\ 0&28&0\\ 28&0&0\\ -3.4&0&0\end{bmatrix}\quad\left[\frac{pm}{V}\right] \quad (20)$$

and $n_1 = n_2 = 2.286$, $n_3 = 2.2$ at an optical wavelength of 633 nm. The drawbacks of $LiNbO_3$ are a moderate figure of merit and a high permittivity of about ε_r=30.

Poled polymers on the basis of Polyimide feature a permittivity of about ε_r=4 and therefore allow a higher penetration of the "static" field but on the other side their figure of merit achieved today is about 5 times lower than for $LiNbO_3$ [13].

C. Sensitivity of the antenna

For the investigation of the sensitivity an optical waveguide of the length L_E consisting of electrooptic material and guiding linear polarized monochromatic light is considered. The change of the intensity reflection coefficient R under the influence of an external electromagnetic field is of primary interest if this waveguide is used as a modulator. The light wave shall be described by:

$$\vec{E}_{opt}=\begin{bmatrix}E_{1,opt}=0\\ E_{2,opt}=0\\ E_{3,opt}\end{bmatrix} \quad (21)$$

and the electromagnetic field by:

$$\vec{E}(x_1)=\begin{bmatrix}E_1(x_1)\\ E_2(x_1)\\ E_3(x_1)\end{bmatrix} \quad (22)$$

correspondingly (see Fig. 10).

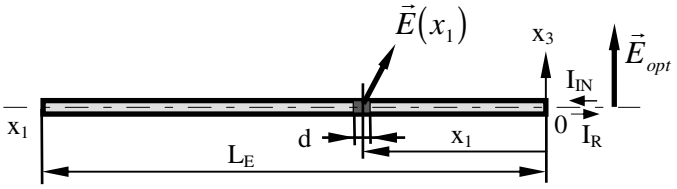

Fig. 10: Electrooptic modulator of length L_E.

Given a material fulfilling eq. 17 and 18, the tensor of the refractive index is reduced to n_3:

$$n_3(E_{1,eff},E_{2,eff},E_{3,eff})=n_3+\Delta n_{3,eff}(E_{1,eff},E_{2,eff},E_{3,eff})$$
with
$$\Delta n_{3,eff}(E_{1,eff},E_{2,eff},E_{3,eff})=$$
$$-\frac{1}{2}\cdot[n_3]^3\cdot[m_{31}\cdot E_{1,eff}+m_{32}\cdot E_{2,eff}+m_{33}\cdot E_{3,eff}] \quad (23)$$
and
$$E_{i,eff}=\frac{1}{L_E}\cdot\int_0^{L_E}E_i(x_i)\cdot dx_i\ ;\ i\in\{1,2,3\}$$

For the operation of the Fabry-Perot etalon the amount of change of the light reflection is of primary interest. From eq. 12 we may deduce:

$$R\left(n_3+\Delta n_{3,eff}(E_{1,eff},E_{2,eff},E_{3,eff})\right)\approx R(r_{21},r_2,t_{12},L_E,\lambda_0,n_3)+$$
$$+\frac{d}{dn_E}R(r_{21},r_2,t_{12},L_E,\lambda_0,n_E)\Big|_{n_E=n_3}\cdot\Delta n_{3,eff}(E_{1,eff},E_{2,eff},E_{3,eff}) \quad (24)$$

Now combining eq. 24 with 11 and 13 and setting $E_{1,eff} = 0$, $E_{2,eff} = 0$ and $n_{E0}=n_3$, an expression for the contrast K_K of the etalon is achieved where the contrast is defined by the second term of eq. 24:

$$I_R=R\cdot[1+K_K]\cdot I_{IN}$$
$$\text{with the contrast}: \quad K_K=\frac{W_S\cdot\frac{\left[[n_3]^3\cdot r_{33}\right]}{\lambda_0}\cdot\int_0^{L_E}E_3(x_1)\cdot dx_1}{R} \quad (25)$$

$$R=R(r_{21},r_2,t_{12},\Lambda)=$$
$$[r_{21}]^2+\frac{2\cdot r_{21}\cdot[t_{12}]^2\cdot r_2\cdot[\cos(\Lambda)+r_{21}\cdot r_2]+[t_{21}]^4\cdot[r_2]^2}{1+[r_{21}\cdot r_2]\cdot 2\cdot\cos(\Lambda)+[r_{21}\cdot r_2]^2} \quad (26)$$

$$W_S=-\frac{[r_{21}\cdot r_2]\cdot\sin(\Lambda)\cdot 4\cdot\pi}{1+[r_{21}\cdot r_2]\cdot 2\cdot\cos(\Lambda)+[r_{21}\cdot r_2]^2}\cdot$$
$$\cdot\left[\frac{2\cdot r_{21}\cdot[t_{12}]^2\cdot r_2\cdot[\cos(\Lambda)+r_{21}\cdot r_2]+[t_{21}]^4\cdot[r_2]^2}{\left[1+[r_{21}\cdot r_2]\cdot 2\cdot\cos(\Lambda)+[r_{21}\cdot r_2]^2\right]}-[t_{12}]^2\right] \quad (27)$$

Λ is defined by eq. 13. Assuming an impinging field E_K inside the dielectric sphere or E_0 outside (see Fig. 1) parallel to the main axis of the probe:

$$\vec{E}_K = -E_K \cdot \vec{e}_z = \frac{3}{\varepsilon_{r,K} + 2} \cdot E_0 \cdot \vec{e}_z$$

and again using prolate spheroidal coordinates, the contrast K_S for a thin ellipsoidal dipole (b/h ≤ 0.05) may be approximated by:

$$\begin{aligned} I_R &= R \cdot [1 \quad + \quad K_S] \cdot I_{IN} \\ K_S(E_K) &= \frac{W_S \cdot M_S \cdot N_S}{R} \cdot E_K \\ N_S &= -\left[\sinh(\eta_0) - \frac{\cosh(\eta_0)}{Q_1(\cosh(\eta_0))} \cdot Q_1'(\cosh(\eta_0)) \right] \\ M_S &= \left[[n_3]^3 \cdot r_{33} \right] \cdot \frac{c}{\lambda_0} \end{aligned} \qquad (28)$$

η_0 is given in eq. 5. The normalized contrast K_{Sn} is defined as:

$$K_{Sn} = \frac{K_S}{M_S \cdot E_K} \qquad (29)$$

A plot of the normalized contrast and the parameter W_S as a function of Λ (see eq. 13) is given in Fig. 11.

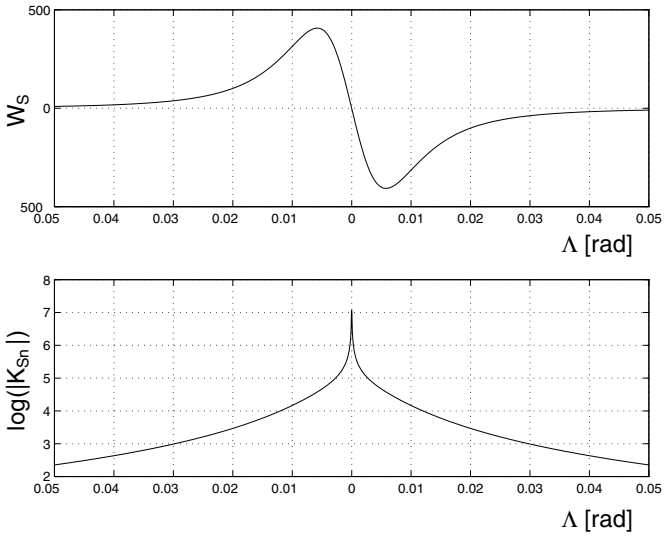

Fig. 11: Behaviour of W_S and K_{Sn} as a function of Λ (measure of the properties of the etalon).

The sensitivity of a probe using for example $LiNbO_3$ for the electrooptic material of the etalon now can be estimated. By selecting an ellipsoidal dipole with b/h = 0.01, a reflectivity of the etalon of r_2 = 0.995 and the normalized contrast $K_{Sn} = 10^5$: The figure of merit for $LiNbO_3$ is about 330 10^{-12} V/m and the permittivity $\varepsilon_{r,K}$= 30. If we choose the optical wavelength λ_0 = 633 nm for the laser source, then we get from eq. 28:

$$K_S = \left[10^5 \cdot 330 \cdot 10^{-12} \cdot 2765 \right] \cdot E_K \quad \approx \quad 0.09 \cdot E_K$$

If we assume in addition that the photodetector is able to detect a minimal contrast K = 0.01, then from eq. 28 we receive the result that a minimum field strength of:

$$E_{K,MIN} \cdot \frac{\varepsilon_{r,K} + 2}{3} = E_{0,MIN} = \frac{0.01}{0.09} \cdot \frac{30 + 2}{3}$$

$$\Rightarrow \quad \underline{\underline{E_{0,MIN} \approx 1 \quad \frac{V}{m}}}$$

can be measured given the parameters mentioned above. This value certainly can be lowered considerably by optimizing the etalon and by applying new materials now under development in different laboratories (see e.g. [14]).

V. Conclusions and Outlook

In this preliminary study about a new electromagnetic field probe resp. receiving antenna using a short dipole and a Fabry-Perot etalon as electrooptic transducers, it has been theoretically proved that very large bandwidths and high sensitivity may be realized. The bandwidth theoretically starts at DC and stops at several GHz depending on the technology applied, all with one probe. Easily realizable is a sensitivity of 1 V/m. For higher sensitivities an optimization of the probe has to be performed, either by applying material for the etalon featuring higher contrast or by choosing a more sophisticated optical receiver. E.g. replacing the photodiode by an optical spectrum analyzer could increase the sensitivity by one to two orders of magnitude. Much research is currently focussed on the improvement of properties of electrooptic materials and it is expected that materials better suited for the application described will be available in the near future (see e.g. [14]).

By using two or more etalons per probe and some signal manipulation at the receiver the cross polarized field components may be suppressed and the sensitivity at least doubled. Furthermore by applying probes in different orientations the vector-field may be picked up. This type of antenna is especially suited for arrays and remote placed antennas at high frequencies.

References

[1] C. Saam: Feld Sensor - Patent Publications**,** SCHAF-R-5; P&TS, Patents & Technology Surveys, Neuchatel, Feb. 20, 2002.

[2] Electric field sensor for controllers of computer, communication apparatus, Japanese patent No JP11194146, March 24, 1998.

[3] K. Hayeiwa, T. Ishikawa, M. Kondo, H. Naka, Y. Sato, Y. Toba: Electric field sensor for electromagnetic wave, e.g. radio receptrion, Japanese patent No JP07306235, May 12, 1994.

[4] Electromagnetic field measuring device has ring laser which is used as electromagnetic field sensor; Japanese patent No JP2001281272, March 3, 2000.

[5] D. P. Hilliard, D. L. Mensa: Photonic EM field sensor for incident planar EM wave; US patent No US5225668, July 6, 1991.

[6] P. A. Schollet: Electric field sensor using Pockels effect on crystal sphere; European patent No EP0453693, Dec. 21, 1990.

[7] H. Frick: Entwicklung eines Feldsensors; ND theses, CTL ETH Zurich, 2002.

[8] H. Frick, G.V. Meyer: An electro-optic E-field sensor. Proc. of the 15th EMC Zurich Symposium, pp. 47 – 52, Feb. 2003.

[9] P. Moon, D. Spencer: Field theory for engineers. Van Nostrand, Princeton, 1961.

[10] B. E. A. Saleh, M. C. Teich: Fundamentals of photonics*;* John Wiley & Sons, INC., 1991.

[11] A. Yariv: Optical electronics in modern communications. 5.Edition, Oxford University Press, 1997.

[12] M. Quillec: Materials for optoelectronics. Kluwer Acadamic Publishers, 1996.

[13] I. Liakatas: Polymer electro-optic modulators: Materials and devices. PhD theses No. 13994, ETH Zurich, 2000.

[14] M.-H. Lee, J. J. Ju, S. Park, J. Y. Do, S. K. Park: Polymer-based devices for optical communications. ETRI Journal, Vol. 24, No. 4, Aug. 2002.